JOURNAL OF VIROLOGY, Sept. 2006, p. 9300–9309 Vol. 80, No. 18
0022-538X/06/$08.00+0 doi:10.1128/JVI.02449-05
Copyright © 2006, American Society for Microbiology. All Rights Reserved.

Poxvirus Tumor Necrosis Factor Receptor (TNFR)-Like T2 Proteins Contain a Conserved Preligand Assembly Domain That Inhibits Cellular TNFR1-Induced Cell Death

Lisa M. Sedger,[1,2]* Sarah R. Osvath,[1] Xiao-Ming Xu,[3] Grace Li,[1] Francis K.-M. Chan,[4] John W. Barrett,[3] and Grant McFadden[3]

Institute for Immunology & Allergy Research and Centre for Virus Research, Westmead Millennium Institute, Department of Medicine, University of Sydney, Sydney, Australia[1]; Department of Molecular Immunology, Immunex Corporation, Seattle, Washington[2]; Department of Microbiology and Immunology, University of Western Ontario, and Robarts Research Institute, London, Ontario, Canada[3]; and Department of Pathology, University of Massachusetts Medical School, Worcester, Massachusetts[4]

Received 22 November 2005/Accepted 23 June 2006

The poxvirus tumor necrosis factor receptor (TNFR) homologue T2 has immunomodulatory properties; secreted myxoma virus T2 (M-T2) protein binds and inhibits rabbit TNF-α, while intracellular M-T2 blocks virus-induced lymphocyte apoptosis. Here, we define the antiapoptotic function as inhibition of TNFR-mediated death via a highly conserved viral preligand assembly domain (vPLAD). Jurkat cell lines constitutively expressing M-T2 were generated and shown to be resistant to UV irradiation-, etoposide-, and cycloheximide-induced death. These cells were also resistant to human TNF-α, but M-T2 expression did not alter surface expression levels of TNFRs. Previous studies indicated that T2's antiapoptotic function was conferred by the N-terminal region of the protein, and further examination of this region revealed a highly conserved N-terminal vPLAD, which is present in all poxvirus T2-like molecules. In cellular TNFRs and TNF-α-related apoptosis-inducing ligand (TRAIL) receptors (TRAILRs), PLAD controls receptor signaling competency prior to ligand binding. Here, we show that M-T2 potently inhibits TNFR1-induced death in a manner requiring the M-T2 vPLAD. Furthermore, we demonstrate that M-T2 physically associates with and colocalizes with human TNFRs but does not prevent human TNF-α binding to cellular receptors. Thus, M-T2 vPLAD is a species-nonspecific dominant-negative inhibitor of cellular TNFR1 function. Given that the PLAD is conserved in all known poxvirus T2-like molecules, we predict that it plays an important function in each of these proteins. Moreover, that the vPLAD confers an important antiapoptotic function confirms this domain as a potential target in the development of the next generation of TNF-α/TNFR therapeutics.

The leporipoxviruses myxoma virus and Shope fibroma virus both encode a high-affinity tumor necrosis factor alpha (TNF-α)-binding protein known as T2 (38, 49). The Shope fibroma virus T2 (S-T2) protein was reported to bind and neutralize both rabbit and human TNF-α (49), but the myxoma virus T2 protein (M-T2) exhibits strict species specificity and inhibits only rabbit TNF-α (38). M-T2 is a genuine virulence factor, because rabbits infected with the M-T2 open reading frame (ORF) knockout myxoma virus vMyxT2G exhibit a markedly attenuated disease compared to rabbits infected with the M-T2-expressing control virus vMyxlac (54). On this basis, M-T2 has served as a model of poxvirus subversion of host immune responses in vitro and in vivo, emphasizing the importance of TNF-α/TNFR biology in the immune response to poxvirus infection (41).

M-T2 also prevents apoptosis of myxoma virus-infected rabbit $CD4^+$ RL5 T cells (24). RL5 cells infected with the T2 knockout vMyxT2G virus die rapidly by apoptosis, thereby precluding optimal virus replication. In contrast, RL5 cells infected with the T2-encoding virus vMyxlac or the vMyxT2R revertant virus do not undergo apoptosis and support productive virus replication (24). However, it is the intracellular version of the M-T2 protein that is required for this antiapoptotic activity because active purified M-T2 protein added to the culture supernatants of vMyxT2G-infected RL5 cells fails to rescue these cells from virus-induced apoptosis (24). Thus, M-T2 has two distinct activities; extracellular or secreted M-T2 binds and inhibits rabbit TNF-α, whereas intracellular M-T2 acts to block virus-infected lymphocyte apoptosis. That M-T2 serves two distinct host evasion functions highlights the intricacies of virus-host interactions (41, 58).

Here, we define the intracellular mechanism of T2's antiapoptotic activity as inhibition of TNFR-mediated cell death. Because myxoma virus and other poxviruses encode a number of other antiapoptotic proteins, including T4 (4), T5 (29), M11L (24), and Serp-2 (28, 33), M-T2 was expressed in mammalian cells in the absence of other poxvirus proteins. M-T2-expressing human Jurkat T cells were found to be resistant to TNF-α- and TNFR-induced cell death, thereby confirming that M-T2 is a bona fide antiapoptotic protein. We demonstrate that M-T2 inhibits human TNFR-induced cell death in a manner that requires a preligand assembly domain (PLAD) located in the N terminus and which is present and conserved in all poxvirus T2-like proteins. We define a novel dominant-negative mechanism of viral subversion of TNF-α/TNFR biology.

* Corresponding author. Mailing address: Westmead Millennium Institute, P.O. Box 412, Westmead, NSW 2145, Australia. Phone: 61-2-9845 7491. Fax: 61-2-9845 9100. E-mail: lisa_sedger@wmi.usyd.edu.au.

MATERIALS AND METHODS

Plasmids. The full-length M-T2 ORF was PCR amplified and cloned into pcDNA3.1myc/his (Invitrogen). pcDNA3-M-T2ΔPLADmyc was constructed by

PCR amplification of the 5′ PLAD-adjacent cDNA spanning the first 54 nucleotides cloned into the BamHI and HindIII sites of pcDNA3.1myc/his and PCR amplification of the 3′ PLAD-adjacent T2 cDNA, beginning at the GGG codon encoding glycine at nucleotide 166, cloned into the HindIII and XhoI sites of pcDNA3.1myc/his. The 5′ pre-PLAD BamHI-HindIII and 3′-post-PLAD HindIII-XhoI M-T2 fragments were then ligated together into BamHI/XhoI-digested pcDNA3.1myc/his. pcDNA3-humanTNFR1 and humanTNFR2 were kindly provided by Chris Benedict (La Jolla Institute for Allergy and Immunology, San Diego, Calif.), and pcDNA3-TNFR1-cyan fluorescent protein (CFP) was generated by Francis Chan and is described elsewhere (8). Full-length p16INK4a was subcloned into pCMV-myc (Clontech) and was kindly provided by Helen Rizos (Westmead Millennium Institute, Westmead, Australia).

Viruses and cells. Control virus vMyxlac, T2 knockout virus vMyxT2G, and T2 revertant virus vMyxT2R were described previously (24, 54). Myxoma virus stocks were grown in BGMK monkey kidney cells (obtained from S. Dales, University of Western Ontario, London, Ontario, Canada) in Dulbecco's modified Eagle's medium (Gibco BRL) with 10% fetal bovine serum (FBS). Recombinant *Autographa californica* nucleopolyhedrosis virus encoding M-T2 (AcM-T2) was constructed by insertion of the M-T2 ORF into the BamHI site of the baculovirus vector, and recombinant baculovirus was propagated in Sf21 cells in TNM medium with 10% FBS or in SF900-II serum-free medium (Gibco BRL). The M-T2 ORF from plasmid pMTN-6 (54) was inserted into the XhoI site of the BMG-neo plasmid and used to generate stable M-T2-expressing human Jurkat T cells by electroporation with a Gene Pulser II instrument (Bio-Rad) at 250 V and 960 μF capacitance. Multiple Jurkat lines constitutively expressing M-T2, designated T2O-a, T2O-11, T2L-4, and T2L-3, were generated by limiting-dilution cloning and expansion in 1 mg/ml G418 (Invitrogen). A BMG-neo plasmid was used to generate the control G418-resistant line JNeo. Jurkat T cells and M-T2-expressing Jurkat lines were cultured in RPMI 1640 medium with 10% FBS; human embryonic kidney (HEK) 293T cells (kindly provided by Grant Logan, Children's Medical Research Institute, Westmead, Australia), Vero cells (originally from the American Type Culture Collection), and U20S human osteosarcoma cells (gift from Helen Rizos, Westmead Millennium Institute, Westmead Australia) were cultured in Dulbecco's modified Eagle's medium with 10% fetal calf serum.

Detection of M-T2 expression in Jurkat cell lines. Jurkat cell RNA, DNA, and protein extracts were prepared with TRIzol reagent (Invitrogen) according to the manufacturer's directions. M-T2-specific oligonucleotide primers were used to confirm T2 DNA incorporation by PCR and M-T2 mRNA expression by reverse transcription-PCR. TRIzol protein extracts were precipitated with isopropyl alcohol, washed with 0.3 M guanidine hydrochloride in ethanol, and pelleted by centrifugation at 7,500 × *g* at 4°C. Secreted M-T2 protein in culture medium was precipitated with 100 μg/ml sodium deoxycholate in 6% trichloroacetic acid for 1 h at 4°C. For controls, BGMK cells were infected with vMyxT2G or vMyxlac at a multiplicity of infection of 10 and harvested 12 or 24 h postinfection.

M-T2-specific antibody B5. M-T2 protein expressed by the recombinant baculovirus AcM-T2 was purified from 20 mM Tris HCl (pH 7.5)-dialyzed culture supernatants with a Hi-trap ion-exchange column (Pharmacia Biotech) equilibrated with 20 mM Tris HCl (pH 7.5) and eluted with a 0 to 1 M linear NaCl gradient. M-T2-containing fractions identified by Western immunoblotting were purified on a Mono-Q column and eluted with a linear 0 to 300 mM NaCl gradient in 20 mM bis-Tris (pH 6.4). Purified M-T2 protein was emulsified in Freund's complete adjuvant and injected intramuscularly into naive New Zealand White rabbits (Riemens Co., St. Agatha, Ontario, Canada) housed at the Robarts Animal Facility in accordance with approved ethics protocols. Rabbits were boosted by a second injection of M-T2 in incomplete Freund's adjuvant and subsequently euthanized and exsanguinated. Serum containing M-T2-specific antibody B5 was affinity purified with an M-T2-conjugated cyanogen bromide-activated Sepharose 4B column (Pharmacia) by standard procedures (20).

Apoptosis assays. Rabbit peripheral blood lymphocytes were isolated from peripheral blood from a healthy naive New Zealand White laboratory rabbit (Riemens Co., St. Agatha, Ontario). Rabbit lymphocytes were isolated from blood by centrifugation over Ficoll-Paque (Amersham Pharmacia Biotech) and separated into nonadherent lymphocytes or adherent monocytes by adherence to plastic petri dishes, exactly as described previously (13). The nonadherent cells, which are primarily lymphocytes, were infected with vMyxlac, vMyxT2G, or vMyxT2R at a multiplicity of infection of 10. Apoptosis of virus-infected cells was detected by terminal deoxynucleotidyltransferase-mediated dUTP-biotin nick end labeling (TUNEL) staining with fluorescein isothiocyanate-conjugated dUTP (Boehringer Mannheim) according to the manufacturer's instructions and as described previously (24). Rabbit lymphocytes were judged to be infected by detecting LacZ expression, staining with 1 mg/ml 5-bromo-4-chloro-3-indolyl-β-D-galactopyranoside (X-Gal) in dimethylformamide, 5 mM potassium ferricyanide, 5 mM potassium ferrocyanide, and 2 mM $MgCl_2$ for 45 min at 37°C and examining cells by light microscopy to detect blue cells. In this situation, LacZ expression is an indication of virus infection and replication because it is expressed by these viruses; the LacZ cDNA has been incorporated into an intergenic region of vMyxlac and hence is also present in the vMyxT2G and vMyxT2R viruses (24).

Jurkat Jneo and M-T2-expressing cell lines were seeded in triplicate, exposed to various inducers of apoptosis, and then incubated with Annexin-V-Fluos (Boehringer Mannheim) and propidium iodide (Sigma) and analyzed by flow cytometry. Specifically, cells were exposed to 10,000 J of UV irradiation, 20 μM etoposide (VP-16; Sigma), and 10 μM cycloheximide (CHX; Sigma) and analyzed by flow cytometry. Additionally, cells were cultured in 30 μM cisplatin or 120 μM melphalan (both from Sigma), LZ-humanTRAIL (TNF-α-related apoptosis-inducing ligand), LZ-humanFasL, LZ-humanCD40L (all from Immunex), or recombinant human TNF-α (R&D Systems), and cell death was assessed by a chromium release assay with a Hewlett-Packard gamma counter. Percent specific lysis was calculated as $x = [(\text{experimental release} - \text{minimum release})/(\text{maximum release} - \text{minimum release})] \times 100$. In some assays, the blocking agents human Fas-Fc, human TRAIL-R2-Fc, and human TNFR1-Fc (Immunex Corporation) were added.

Flow cytometric measurement of TNFR expression and TNF-α binding. For surface and intracellular staining, Jurkat cells were incubated for 1 h at 4°C with 5% normal human serum and then incubated with 10 μg of the following antibodies: mouse immunoglobulin G1 (IgG1) M180 anti-huTRAIL, mouse IgG1 M271 anti-huTRAILR1, mouse IgG1 M413 anti-huTRAILR2, mouse IgG1 M430 anti-huTRAILR3, mouse IgG1 M444 anti-huTRAILR4, mouse IgG1 M38 anti-Fas, or isotype control antibody mouse IgG1 M330 anti-RANK (receptor activator of NFκB) IgG1, which were described previously (12, 18, 43). Binding of primary antibodies was detected by incubation with biotinylated F(ab′)2 goat anti-murine IgG (Jackson Laboratories) and avidin-phycoerythrin (Av-PE; Pharmingen). Jurkat cells and transfected 293T cells were also incubated in PE-conjugated mouse IgG1 (clone 16803.1) anti-human TNFR1, PE-conjugated mouse IgG2a anti-human TNFR2 (clone 22235), PE-conjugated mouse IgG1 (clone 11711), or PE-conjugated mouse IgG2a (clone 20102) isotype control antibodies, according to the manufacturer's instructions (all from R&D Systems). For intracellular staining, cells were fixed in 2% paraformaldehyde in phosphate-buffered saline (PBS) for 10 min at 4°C and stained and washed in 0.1% saponin (Sigma).

For TNF-α binding, HEK 293T cells were transfected with pcDNA3-TNFR1 and either pcDNA3-M-T2myc or pcDNA3-M-T2ΔPLADmyc or with each plasmid alone, incubated 24 h later in recombinant human TNF-α (R&D Systems) for 10 min at 4°C or room temperature, and washed three times in PBS with 5% fetal calf serum to remove unbound TNF-α. Remaining bound TNF-α was detected by flow cytometry with anti-human TNF-α–PE antibody (clone 6402.31; R&D Systems) and compared to staining with isotype control PE-conjugated mouse IgG1 (clone 11711; R&D Systems). The expression of ectopically expressed TNFRs in these experiments was also checked by flow cytometry with the PE-conjugated TNFR-specific antibodies listed above. Cells were analyzed on a FACScan or FACScalibur flow cytometer (Becton Dickenson), and 10,000 or 30,000 events were collected and analyzed with Cell Quest system software (BD Biosciences).

Transfection and immunoprecipitation studies. For viability studies, HEK 293T cells seeded in six-well tissue culture plates were transfected with various combinations of pcDNA3.1myc/his, pcDNA3-M-T2myc/his, pcDNA3-T2ΔPLADmyc/his, and pcDNA3-TNFR1, together with pcDNA3-LacZ, by a calcium phosphate transfection method described previously (17). β-Galactosidase activity was quantitated as follows. Lysates were prepared by three cycles of freezing-thawing on dry ice and centrifugation at 13,000 rpm for 15 min to remove debris and then incubated with *o*-nitrophenyl-β-D-galactopyranoside in 0.1 M $MgCl_2$ plus 5 mM β-mercaptoethanol in 0.1 M sodium phosphate buffer (pH 7.3), and LacZ expression was measured by absorbance at 415 nm with a Titertek Multiskan plate reader.

For immunoprecipitation studies, HEK 293T cells seeded in 10-cm dishes were transfected with pcDNA3-TNFR1 or pcDNA3-TNFR2 and either pcDNA3-M-T2myc, pcDNA3-M-T2ΔPLADmyc, or pcDNA3 (empty vector) and 48 h later harvested directly into RIPA buffer containing complete protease inhibitors (Roche). Lysates were precleared with a 50/50 mixture of a protein A and protein G-Sepharose (Sigma) slurry in PBS. Beads were pelleted by centrifugation, and supernatants were incubated with protein A/G-Sepharose plus 1 μl of rabbit anti-human TNFR1 antibody (H5; Santa Cruz) or 1 μl of goat anti-human TNFR2 antibody (C20; Santa Cruz) and incubated overnight at 4°C with rotation. Beads were washed three times, resuspended in sodium dodecyl sulfate-polyacrylamide gel electrophoresis (SDS-PAGE) reducing sample buffer, and examined by SDS-PAGE and immunoblotting. Briefly, samples were subjected

to 12% SDS-PAGE, blotted onto polyvinylidene difluoride membrane (Bio-Rad), incubated overnight in 10% skim milk in PBS plus 5% Tween 20 to block nonspecific binding, then incubated with B5 anti-M-T2 rabbit serum and biotinylated goat anti-rabbit antibody (Sigma), and developed with 5-bromo-4-chloro-3-indolyl-β-D-galactopyranoside (BCIP)–nitroblue tetrazolium alkaline phosphatase substrate (Sigma). Alternatively, lysates were analyzed directly by immunoblotting with B5 anti-M-T2, H5 anti-TNFR1, or C20 anti-TNFR2 antibody (Santa Cruz).

M-T2myc and M-T2ΔPLADmyc binding to human and rabbit TNF-α was also determined by immunoprecipitation. In these experiments, TNF-α binding was determined by mixing 500 μg of total protein from pcDNA3.1, pcDNA3.1-M-T2myc, and pcDNA3.1-M-T2ΔPLADmyc transfected HEK 293T cells with lysates and supernatants from Vero cells infected with vaccinia viruses (VV) encoding human or rabbit TNF-α, which have been described previously (39). In these assays, M-T2myc and M-T2ΔPLADmyc were mixed with anti-c-Myc antibody (clone 9E10; Santa Cruz) overnight at 4°C. Antibody-bound M-T2 complexes containing TNF-α were then immunoprecipitated with protein G-Sepharose beads (Upstate) for 1 h. Sepharose beads were washed four times in lysis buffer containing 0.5% deoxycholate and proteinase inhibitor cocktail (Roche), and immunoprecipitates were subjected to SDS-PAGE. TNF-α was detected by Western immunoblotting with the TNF-α-specific antibodies rabbit anti-human TNF-α (BioSource International) and goat anti-rabbit TNF-α (Fitzgerald Industries). These antibodies were detected with goat anti-rabbit immunoglobulin and donkey anti-goat immunoglobulin secondary antibodies, respectively (both from Jackson Immunoresearch). Immunoblots were visualized with Western Lightning chemiluminescence reagent plus (Perkin-Elmer).

Confocal microscopy. Confocal microscopy was performed on U2OS cells seeded onto 13-mm round glass coverslips that were placed in six-well tissue culture dishes. pcDNA3-TNFR1-CFP and pcDNA3-M-T2myc or pcDNA3-M-T2ΔPLADmyc transfected U203 cells were fixed in 2% paraformaldehyde at 24 h posttransfection. M-T2myc and M-T2ΔPLADmyc proteins were detected by staining with rabbit anti-myc antibody (clone 9E10; Santa Cruz) and then goat anti-rabbit immunoglobulin Cy3-labeled antibody (Amersham Pharmacia Biotech) in 0.1% saponin–PBS. TNFR1-CFP and T2myc were visualized in U20S cells with a Leica SP2 confocal microscope with helium neon and argon lasers. Images were captured with Leica confocal software.

Statistical analysis. Where appropriate, data were analyzed statistically by a two-tailed Student *t* test. A P value of <0.05 was considered statistically significant.

RESULTS

M-T2 protects primary rabbit lymphocytes from virus-induced apoptosis. M-T2 can protect rabbit RL5 $CD4^+$ T lymphocytes from virus-induced apoptosis (24). In order to determine whether this is a biologically relevant phenomenon or a peculiarity of this rabbit cell line, primary rabbit lymphocytes were examined. Rabbit peripheral blood leukocytes were collected, lymphocytes were separated from monocytes by adherence to plastic, and the nonadherent lymphocytes were infected with the M-T2-deficient vMyxT2G virus or the parental M-T2-expressing control virus and assessed by flow cytometry by fluorescein isothiocyanate-dUTP (TUNEL) staining. Infection with vMyxT2G resulted in an increase in apoptotic cells in primary blood lymphocytes, in that there were 14% TUNEL-positive cells in vMyxLac-infected leukocytes, but this was increased to 26% in vMyx-T2G-infected leukocytes at 24 h postinfection (data not shown). Primary rabbit lymphocytes were judged to be infected because approximately 70% of rabbit lymphocytes were expressing LacZ, which is encoded by these viruses (data not shown). Thus, M-T2 inhibits apoptosis of primary rabbit blood lymphocytes (data not shown), not just that of the transformed rabbit RL5 T-cell line (24).

Expression of M-T2 from stably transfected Jurkat clones. Myxoma virus encodes a number of gene products that can inhibit apoptosis (for a review, see reference 31). In order to characterize the antiapoptotic properties of M-T2 in lymphocytes and to circumvent the limitations of secreted M-T2's ability to neutralize only rabbit TNF-α and not human TNF-α (38), we expressed M-T2 in human Jurkat T cells in the absence of virus infection. Human $CD4^+$ Jurkat T-cell clones T2O-a, T2O-11, T2L-4, and T2L-3 were generated and found to express M-T2-specific mRNA (data not shown). M-T2 protein was judged to be properly synthesized in each of these lines, as both lysates and culture supernatants contained the 55-kDa M-T2 protein (Fig. 1A and data not shown). No M-T2 protein was present in Jneo control cells (Fig. 1A). Since the intracellular form of M-T2 was required for protection against apoptosis (24), the relative amount of intracellular M-T2 expressed by the Jurkat clones was quantitated by immunoblotting and densitometry. Jurkat clone T2O-a expressed the highest level of intracellular M-T2, followed by Jurkat clone T2O-11 and then clones T2L-4 and T2L-3 (Fig. 1A). Thus, M-T2 was efficiently expressed in human Jurkat lymphocytes in the absence of virus infection and without DNA codon optimization. Importantly, detection of M-T2 protein in both lysates and supernatants of the Jurkat clones is completely analogous to the normal expression of M-T2 or S-T2 during virus infection or when expressed via plasmid transfection in rabbit RK13 fibroblasts (2, 53; L. Sedger, unpublished data).

M-T2 inhibits TNF-α-mediated apoptosis. Next, we investigated whether Jurkat T cells expressing M-T2 are more resistant to apoptosis induced by different stimuli. To determine whether M-T2 blocks UV-induced apoptosis, control Jneo Jurkat cells and M-T2-expressing Jurkat cells were exposed to 10,000 J of UV irradiation, which induced 32% of the Jneo cells tested to undergo apoptosis (Fig. 1A). In contrast, only 9% of Jurkat T2O-a cells, 14% of Jurkat T2O-11 cells, 16% of Jurkat T2L-4 cells, and 22% of Jurkat T2L-3 cells underwent apoptosis after UV irradiation (Fig. 1A). In order to determine whether M-T2 also protects Jurkat T cells against other inducers of apoptosis, these cells were tested for sensitivity to etoposide (VP-16) and CHX. All M-T2-expressing Jurkat cells were more resistant to VP-16- and CHX-induced apoptosis compared to Jneo control cells, and the cells that had the highest M-T2 expression (T2O-a) also exhibited the greatest resistance (Fig. 1A). M-T2-expressing Jurkat T-cell clones were also tested for sensitivity to the UV-mimetic agents cisplatin and melphalan. Death induced by these agents is much slower, and hence, 24-h and 48-h ^{51}Cr release assays were used to measure apoptosis. However, Jurkat lines expressing M-T2 were not more resistant to these cytotoxic agents than Jneo control cells (data not shown). Together, these data indicate that M-T2 expressed in the absence of myxoma virus infection induced resistance to UV irradiation-, VP-16-, and CHX-induced cell death but not cisplatin- or melphalan-induced cell death.

UV irradiation is known to induce TNF-α production and also increase the expression and aggregation of TNFR in keratinocytes and other cell lines (3, 23, 50), whereas the UV-mimetic agents cisplatin and melphalan do not (46). Moreover, caspase-$8^{-/-}$ cell lines are reportedly more resistant to apoptosis induced by both UV irradiation and etoposide (22). Therefore, M-T2-expressing Jurkat clones were tested for the ability to resist apoptosis induced by TNF-α and other caspase-8-sensitive death receptor-binding cytokines TRAIL and FasL. Recombinant human TNF-α, LZ-TRAIL, LZ-FasL, and LZ-

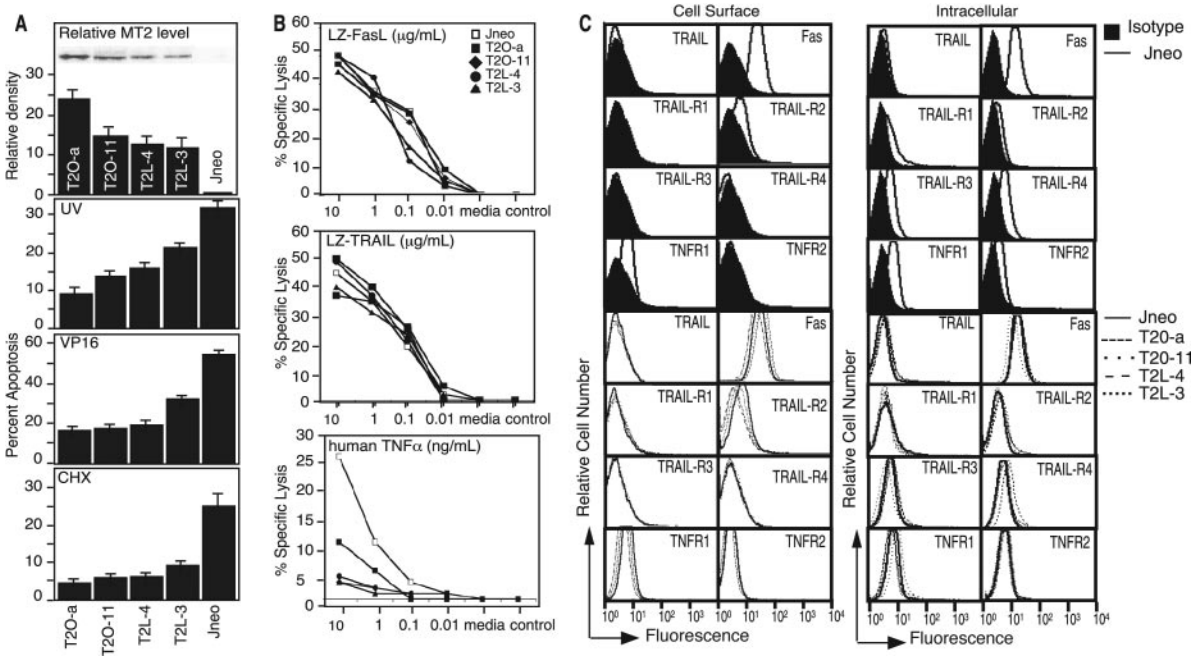

FIG. 1. Expression of M-T2 in stably transfected Jurkat T-cell lines and susceptibility to apoptosis. (A) M-T2 expression in stably transfected Jurkat T-cell clones T2O-a, T2O-11, T2L-4, T2L-3, and Jneo analyzed by Western immunoblotting and densitometry. Percent apoptosis induced in M-T2-expressing and control Jurkat T cells after exposure to 10,000 J of UV irradiation, 20 μM etoposide (VP-16), and 10 μM CHX for 8 h. Data shown are means ± standard deviations and are representative of replicate experiments. (B) Susceptibility of Jneo (unfilled squares) and M-T2-expressing Jurkat T cells (filled symbols) after 8 h of culture in LZ-TRAIL, LZ-FasL, LZ-CD40L (control), or recombinant human TNF-α. Data are means ± standard errors of the means, which were ≤5%, and error bars have been omitted for clarity. (C) Flow cytometry analysis of death receptor expression in Jurkat T-cell clones. Histograms show death receptor expression on the control Jneo Jurkat line (solid lines), both at the cell surface and intracellularly, relative to staining with isotype control antibodies (filled histograms). Death receptors on M-T2-expressing Jurkat lines T2O-a (dots), T2O-11 (spaced dots), T2L-4 (small dashes), and T2L-3 (large dashes) are overlaid with control Jneo cells (solid lines).

CD40 (control) were used because they induce ligand-mediated receptor-specific signaling (56). In an 8- or 18-h ^{51}Cr release assay, all M-T2-expressing Jurkat clones were significantly more resistant to TNF-α-mediated death compared to control Jneo cells (Fig. 1B and data not shown), but they were not more resistant or susceptible to LZ-FasL or LZ-TRAIL, and as expected, there was no proapoptotic effect by the control reagent LZ-CD40L (Fig. 1B). Thus, M-T2 expression conferred specific protection from human TNF-α-mediated cell death, which is consistent with resistance to UV, etoposide, and CHX, which inhibit the synthesis of antiapoptotic proteins such as inhibitors of apoptosis.

Ectopic expression of M-T2 does not alter the expression of TNFR, Fas, or TRAIL receptors. The finding that M-T2-expressing Jurkat clones were more resistant to human TNF-α was surprising because secreted M-T2 binds to and inhibits only rabbit TNF-α and not human TNF-α (38). Thus, we reasoned that forced expression of M-T2 might have influenced TNFR expression on Jurkat cell lines, potentially explaining these results. Therefore, death receptor-specific monoclonal antibodies and flow cytometry were used to assess TNFR family molecule expression levels on control Jneo cells and M-T2-expressing Jurkat lines T2-Oa, T2O-11, T2-L3, and T2-L3. First, Jneo cells were assessed and found to express detectable surface levels of Fas but only low levels of surface TRAIL-R2 and TNFR1 and no surface TRAIL, TRAIL-R1, TRAIL-R3, TRAIL-R4, or TNFR2 relative to staining with isotype control antibodies. All M-T2-expressing Jurkat cells expressed essentially similar levels of these molecules at the cell surface, with only a very minimal reduction in surface TNFR1 (Fig. 1C). The intracellular levels of death receptors found in each of these cell lines were also assessed with permeabilized cells; however, none of these molecules, including TNFR1 and TNFR2, were significantly altered in M-T2-expressing Jurkat lines (Fig. 1C). Thus, M-T2 expression did not significantly alter surface or intracellular TNFR molecule expression levels.

Poxvirus T2 ORFs contain a highly conserved PLAD. The N-terminal cysteine-rich repeat domain (CRD)-containing region of the myxoma virus and S-T2 ORFs are highly similar to human TNFR (41), and previous mutational studies had indicated that the N-terminal region of M-T2 contains distinct domains responsible for TNF-α binding and inhibition of virus-induced apoptosis (40). Further analysis of the first 200 N-terminal amino acids of the M-T2 and S-T2 proteins and human TNFR1 and TNFR2 identified a highly conserved region in M-T2 and S-T2 which resides within the first CRD (8) and has clear homology to the PLAD of human TNFRs (Fig. 2). The human TNFR PLAD is important in conferring a conformation change in the structure of TNFRs and allows TNFR self-association prior to ligand binding and signaling (8). As such, the PLAD is required for signaling competency. This vPLAD is present in all poxvirus T2-like molecules: myxoma virus M-T2 (Lausanne strain; accession no. NC_001132) (7), Shope fibroma virus S-T2 (Kasza strain; accession no.

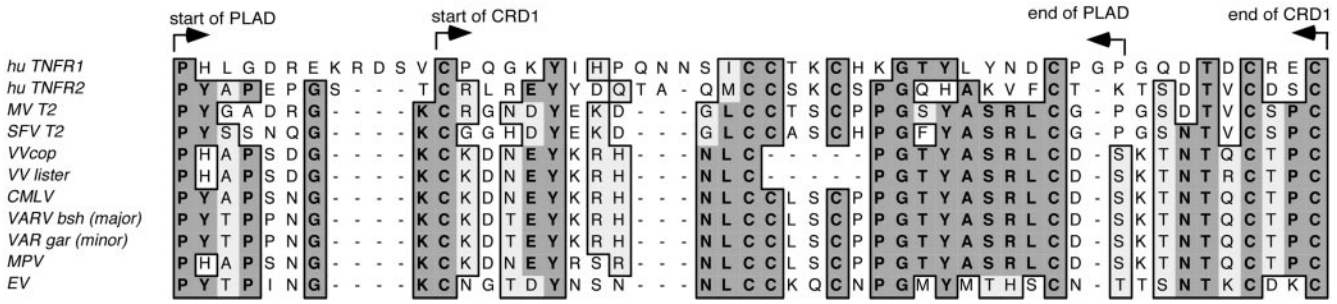

FIG. 2. Poxvirus T2-like molecules contain a conserved PLAD. Sequence similarity analysis of the N-terminal region of the myxoma virus (MV), Shope fibroma virus (SFV), VV strain Lister and Copenhagen, camelpox virus (CMLV), variola major virus strain Bangladesh (VAR bsh major), variola minor virus strain Garcia (VAR gar minor), monkeypox virus (MPV), and ectromelia virus (EV) T2 ORFs and human TNFR1 and TNFR2 reveals a highly conserved PLAD that overlaps the first CRD. Identical amino acids (bold) and conserved amino acid differences (gray) are indicated.

NC_001266) (57), camelpoxvirus CMLV002 and CMLV210 (Kazakhstan M-96 strain; accession no. NC_003391) (1), variola minor virus G2R (strain Garcia; accession no. Y16780) (45), variola major virus G2R (strain Bangladesh-1975; accession no. L22579) (26), monkeypox virus J2L (strain Zaire 96-1-16; accession no. NC_003310) (44), ectromelia virus CrmD (strain Moscow; accession no. NC_004105) (9), and even the fragmented T2-like ORFs in VV (strains Lister; accession no. U86871 [V. N. Loparev, J. M. Parsons, and J. J. Esposito, unpublished data], and Copenhagen; accession no. NC_001559) (16) (Fig. 2). In fact, there is 22 to 37% amino acid identity and 27 to 47% amino acid similarity between human TNFR1 and TNFR2 PLAD/CDR1 and the vPLAD present in poxvirus T2-like ORFs (Fig. 2 and data not shown). Hence, all known viral T2 family ORFs contain a highly conserved vPLAD that overlaps the first CRD in viral and cellular TNFR molecules.

M-T2 inhibits TNFR1-mediated apoptosis acting via its conserved vPLAD. Because M-T2 specifically inhibited Jurkat T cells from human TNF-α-mediated apoptosis (Fig. 1B) and since secreted M-T2 does not bind or inhibit human TNF-α (38) nor influence endogenous human TNFR expression levels (Fig. 1C), we hypothesized that M-T2 functions as a dominant-negative TNFR inhibitor molecule (31, 41). To determine whether M-T2 specifically inhibits TNFR1-induced death and the relative importance of this vPLAD, a series of cotransfection experiments were performed with full-length M-T2 or a T2 mutant in which the vPLAD was deleted (M-T2ΔPLAD). Plasmid pcDNA3-M-T2myc, pcDNA3-M-T2ΔPLADmyc, or pcDNA3 was cotransfected with pcDNA3-TNFR1 and pcDNA3-LacZ, and TNFR-induced cell death was assayed by measuring β-galactosidase activity in surviving HEK 293T cells. Overexpression of TNFR1 alone (or with an empty control plasmid) induced significant cell death ($P = 0.001$) compared to pcDNA3, and most cells appeared rounded and became detached from the culture dish. In contrast, expression of full-length M-T2myc significantly inhibited TNFR1-induced HEK 293T cell death ($P = 0.001$) (Fig. 3 and data not shown). In all T2-cotransfected cultures, 293T cells appeared healthy, as judged by phase-contrast microscopy (data not shown). In contrast, M-T2ΔPLADmyc did not protect 293T cells from TNFR1-induced death, and in fact, M-T2ΔPLADmyc conferred increased sensitivity to TNFR1-induced death ($P = 0.01$) for reasons that are unclear (Fig. 3). As expected, both M-T2myc and M-T2ΔPLADmyc proteins were detected in transfected 293T cells (Fig. 3, insert), and interestingly, M-T2myc also inhibited transfection-induced HEK 293T cell death (Fig. 3), perhaps implying that the transfection procedure itself induces TNF-α and/or TNFR-mediated cell death. Moreover, S-T2 similarly inhibited human TNFR1-induced cell death even in the presence of saturating amounts of purified human TNFR1-Fc, which was added to the culture supernatants to sequester any possible production of transfection-induced TNF-α (data not shown). Thus, leporipoxvirus T2 proteins inhibit human TNFR1-induced death in vitro, and for M-T2, this activity requires an intact vPLAD.

M-T2 physically associates with TNFR1 and TNFR2. Due to the highly conserved N-terminal region of leporipoxvirus T2 with human cellular TNFRs (41), we hypothesized that M-T2 inhibited TNFR signaling by directly interacting with TNFRs themselves, forming an inhibitory heterocomplex (31, 41). To determine whether M-T2 specifically interacts with human TNFRs, cotransfections were again performed and TNFR1 or

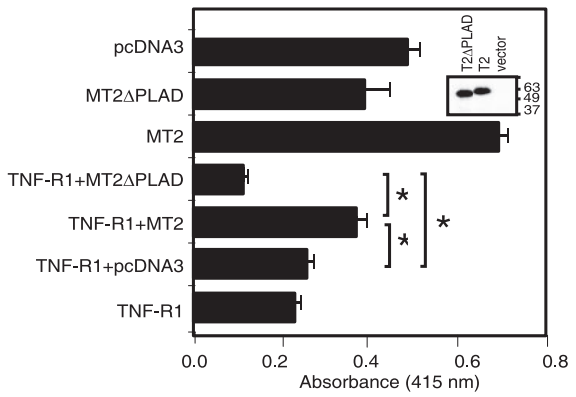

FIG. 3. T2 protects against TNFR1-induced cell death. Survival of HEK 293T cells 48 h posttransfection with pcDNA3-TNFR1 and pcDNA3-M-T2myc or pcDNA3-M-T2ΔPLADmyc together with LacZ, and other control plasmids, as indicated. Viability was determined by measuring β-galactosidase activity in surviving cells. Data shown are means ± the standard errors of the means of triplicate transfections, each measured in quadruplicate, and are representative of repeated assays. An asterisk indicates a statistically significant difference ($P < 0.05$). (Insert) Western immunoblot detection of M-T2myc and M-T2ΔPLADmyc in transfected HEK 293T cells.

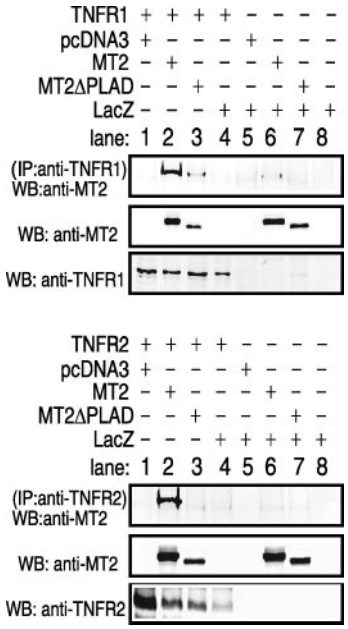

FIG. 4. Immunoprecipitation analysis of M-T2 and TNFR. HEK 293T cells were cotransfected with pcDNA3-TNFR1 or pcDNA3-TNFR2 and either pcDNA3-M-T2myc, pcDNA3-T2ΔPLADmyc, or pcDNA3-LacZ. TNFR1 was immunoprecipitated with anti-TNFR1-specific H5 antibody, TNFR2 was immunoprecipitated with TNFR2-specific C20 antibody, and TNFR-associated M-T2 was detected with anti-M-T2 B5 antibody. IP, immunoprecipitation; WB, Western immunoblotting.

TNFR2 was immunoprecipitated and examined for the presence of associated M-T2myc or M-T2ΔPLADmyc protein. Antibodies specific to either TNFR1 or TNFR2 bound to a TNFR complex that contained M-T2myc (Fig. 4). In contrast, the T2 mutein T2ΔPLADmyc interacted considerably less well and not at all with TNFR1 and TNFR2, respectively (Fig. 4). Analogous experiments also demonstrated that S-T2 physically associates with human TNFRs (data not shown). Taken together, these data indicate that leporipoxvirus T2 physically associates with human TNFR1 and TNFR2 and that the interaction largely requires the presence of the vPLAD.

Intracellular localization of the M-T2-TNFR1 complex. To determine where M-T2 physically associates with TNFRs, we examined TNFR and T2 expression by confocal microscopy. For this, the TNFR1-CPF and M-T2myc or M-T2ΔPLADmyc proteins were coexpressed by transfection into U20S human osteosarcoma cells and examined for CFP (TNFR1) expression and M-T2myc expression with a Cy3-tagged anti-myc antibody. TNFR1-CFP was clearly detectable intracellularly in a compartment resembling the Golgi apparatus, which is consistent with the fact that most TNFR1 protein is found in intracellular compartments within cells and specifically in the trans-Golgi (21). Although M-T2 was historically described as a secreted protein (54), it was clearly detectable within lysates from virus-infected cells or cDNA-transfected 293T cells (Fig. 3 and data not shown), and confocal-microscopy examination demonstrated that M-T2myc and M-T2ΔPLADmyc are abundantly present intracellularly in transfected U20S cells (Fig. 5 and data not shown). Furthermore, M-T2myc and

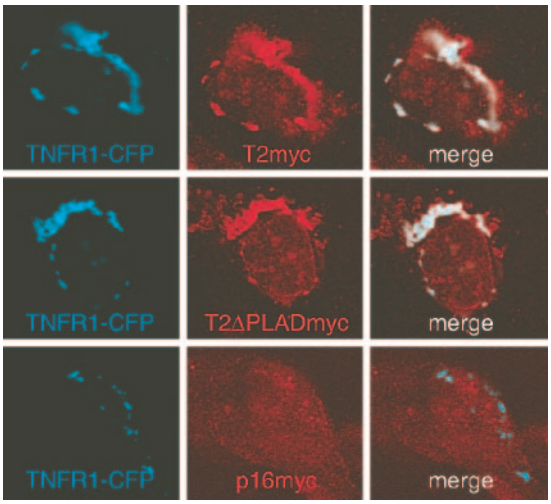

FIG. 5. Intracellular localization of the M-T2-TNFR1 complex. Confocal-microscope detection of human TNFR1-CFP, M-T2myc (Cy3), or p16INKmyc (Cy3) in cotransfected U20S cells. Cells were fixed with 2% paraformaldehyde, permeabilized in 0.1% saponin, stained, and examined at 24 h posttransfection with a Leica SP2 confocal microscope. Shown are CFP fluorescence, Cy3 fluorescence, and merged images of both. Results are representative of repeated experiments.

M-T2ΔPLADmyc clearly colocalized with TNFR1-CFP within intracellular compartments (Fig. 5, merge panels). For control purposes, U20S cells were also cotransfected with pcDNA3-TNFR1-CPF and pCMV-p16INK4a. p16INK is found as a diffuse cytoplasmic protein (34), and although both p16INK and TNFR1-CFP are clearly expressed, p16INK does not colocalize with TNFR1-CFP (Fig. 5, merge panel). Hence, M-T2's inhibition of TNFR1-induced cell death occurs by virtue of its association with TNFR1, and these proteins are clearly found localized together within cells.

Cell-associated M-T2 and TNF-α binding. Finally, we tested whether the presence of cell-associated M-T2 impeded the binding of human TNF-α. For this, HEK 293T cells were transfected with TNFR1 and M-T2myc or M-T2ΔPLADmyc or with TNFR2 and M-T2myc or M-T2ΔPLADmyc and 24 h later, incubated with recombinant human TNF-α for 10 min at 4°C. Bound TNF-α was then detected by flow cytometry. Cell surface-bound TNF-α was detectable at equal levels in cells expressing TNFR1, TNFR1 and M-T2myc, or TNFR1 and M-T2ΔPLADmyc (Fig. 6A). Surface TNF-α binding was also unaltered in 293T cells expressing TNFR2, TNFR2 and M-T2myc, or TNFR2 and M-T2ΔPLADmyc (Fig. 6A). Importantly, TNFR1 is only present at low levels at the cell surface compared to TNFR2, which is abundantly present after transfection (Fig. 6A). Therefore, at least for TNFR1-expressing cells, TNF-α binding is likely to have reached saturation, and hence coexpression of M-T2 does not impinge on human TNF-α binding to this receptor. However, in order to accurately interpret these data we investigated whether M-T2myc is detectable at the cell surface. Confocal-microscopic examination of U20S cells transfected with TNFR1-CPF and M-T2myc clearly detected M-T2myc at the cell surface, that is, on unpermeabilized cells, but it is uncertain whether M-T2myc and TNFR1-CFP colocalize at the cell surface, because all intra-

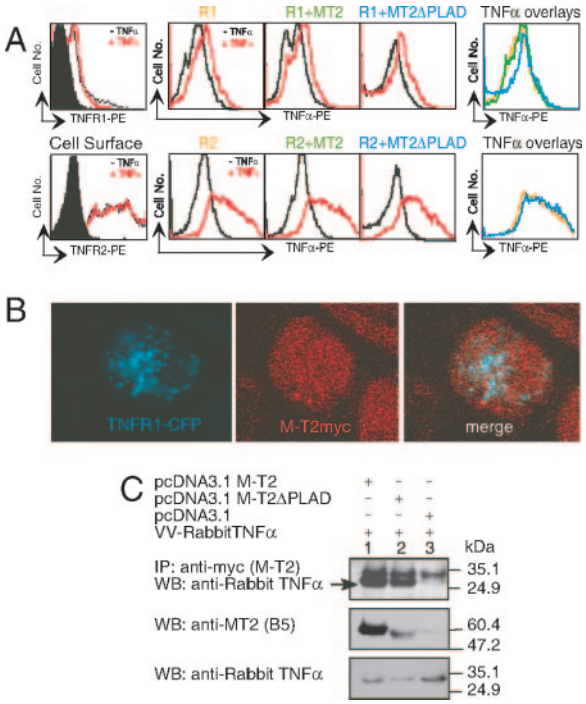

FIG. 6. Cell-associated M-T2 and TNF-α-binding. (A) Flow cytometry analysis of human TNF-α binding to the surface of HEK 293T cells transfected with TNFR1, TNFR1 plus M-T2myc, or TNFR1 plus M-T2ΔPLADmyc (top row) or with TNFR2, TNFR2 plus M-T2myc, or TNFR2 plus M-T2ΔPLADmyc (second row) at 24 h posttransfection. Shown is the surface fluorescence of bound TNF-α, detected with anti-human TNF-α–PE antibody, after 10 min of culture with (red, unfilled histograms) or without (black, unfilled histograms) recombinant human TNF-α. Isotype control staining (filled histograms) and surface expression levels of TNFR1 and TNFR2 24 h after transfection are also shown, as are overlays of TNF-α staining in each transfection (orange, TNFR; green, TNFR plus M-T2; blue, TNFR plus M-T2ΔPLAD). Data shown are representative of independently repeated experiments. (B) Surface detection of TNFR1-CFP and M-T2myc protein at 24 h posttransfection on unpermeabilized U20S cells (TNFR1-CFP, M-T2myc [Cy3], and merged images of both). (C) Cell-associated M-T2myc and M-T2ΔPLADmyc binding to rabbit TNF-α. M-T2myc- and M-T2ΔPLADmyc-containing HEK 293T transfected-cell lysates were mixed with Vero cell lysates containing rabbit TNF-α expressed by recombinant VV. M-T2myc-bound rabbit TNF-α was detected by immunoprecipitation (IP) with anti-myc antibody and Western immunoblotting (WB) with rabbit TNF-α-specific antibody (as indicated). Expression of M-T2, M-T2ΔPLAD, and rabbit TNF-α was confirmed by Western immunoblotting.

cellular CFP-labeled TNFR1 protein is detected in this assay (Fig. 6B). Hence, M-T2 is detectable at the cell surface but does not interfere with human TNF-α binding to human TNFR1 or human TNFR2 (Fig. 6A and B). Moreover, that TNF-α binding is unaltered in HEK 293T cells expressing M-T2myc alone (data not shown) or M-T2 plus TNFR1 or M-T2 plus TNFR2 (Fig. 6A) implies that cell-associated M-T2myc does not itself bind human TNF-α. To confirm that cell-associated M-T2 only binds rabbit TNF-α, we performed a mixing experiment in which lysates from pcDNA3-M-T2myc and pcDNA3-M-T2ΔPLADmyc transfected 293T cells were combined with lysates from Vero cells infected with recombinant VV encoding VV-rabbit TNF-α or VV-human TNF-α. In these experiments, immunoprecipitated M-T2myc and M-T2ΔPLADmyc bound rabbit TNF-α, as expected (Fig. 6C), but human TNF-α was not detected in complex with immunoprecipitated M-T2myc or M-T2ΔPLADmyc (data not shown). This is consistent with our previous reports that secreted M-T2 binds TNF-α in a species-specific manner; that is, it binds rabbit TNF-α but not mouse or human TNF-α (38, 39). Furthermore, these results confirm our previous findings that the TNF-α-binding and antiapoptotic functions of M-T2 are conferred by different domains, both within the N-terminal TNFR-homologous region of M-T2 (37, 40, 41). Taken together, these data indicate that M-T2 is a bone fide antiapoptotic protein that acts by virtue of its ability to physically associate with cellular TNFRs in intracellular compartments and through its highly conserved vPLAD. Thus, cell-associated M-T2 inhibits TNF-α and TNFR1 signaling in a species nonspecific manner by forming a dominant-negative intracellular receptor complex, and this is independent of secreted M-T2's documented ability to bind and inhibit soluble TNF-α, which is species specific.

DISCUSSION

We have demonstrated that leporipoxvirus M-T2, a viral TNFR homologue, is a genuine antiapoptotic factor that can inhibit human TNFR1-mediated apoptosis independently of its known ability to bind rabbit TNF-α, and in the absence of any other myxoma virus protein. Moreover, we demonstrated that the ability of M-T2 to inhibit TNFR1-induced cell death is dependent on an N-terminal PLAD-homologous domain within T2 (vPLAD) and involves the formation of an intracellular TNFR–M-T2 heterocomplex. This complex appears to work by preventing TNFR signaling rather than by impeding TNF-α binding to cellular TNFRs at the cell surface.

Although it is clear that poxviruses have evolved multiple strategies to prevent apoptosis, including the specific ability to inhibit secreted TNF-α (39, 54), we have described a mechanism of viral inhibition of TNFR-mediated apoptosis that appears to be unique (42). It is different mechanistically from the actions of the myxoma virus ubiquitin ligase M153R gene product that down-regulates Fas from the surface of infected cells (19, 25), and unlike the adenovirus receptor internalization domain (RID) proteins that specifically interact with Fas, TNFRs, and TRAIL-Rs, forcing their internalization and degradation (15, 47, 51, 52). Moreover, there are no similarities to other previously described antiapoptotic strategies utilized by lymphotropic viruses (27). Although the papillomavirus E6 protein can specifically inhibit TNFR signaling without decreasing surface TNFR expression (14), there are no functional or amino acid sequence similarities between T2 and E6. Thus, these proteins appear to act via distinctly different mechanisms: papillomavirus E6 inhibits apoptosis by binding to the intracellular region of human TNFR, preventing the association of TRADD and FADD (14), while M-T2 acts via its N-terminal vPLAD to form a dominant-inhibitory T2-TNFR complex (Fig. 3 and 4). Furthermore, the ability of M-T2 to inhibit human TNF-α function by preventing cellular TNFR signaling while not impeding TNF-α binding to cellular TNFRs (Fig. 6) highlights how this mechanism of subverting TNF-α prevents any potential exacerbation of immunopathological effects of TNF-α. Indeed, because the cellular TNFRs can still bind human TNF-α there is not likely to be an increase in

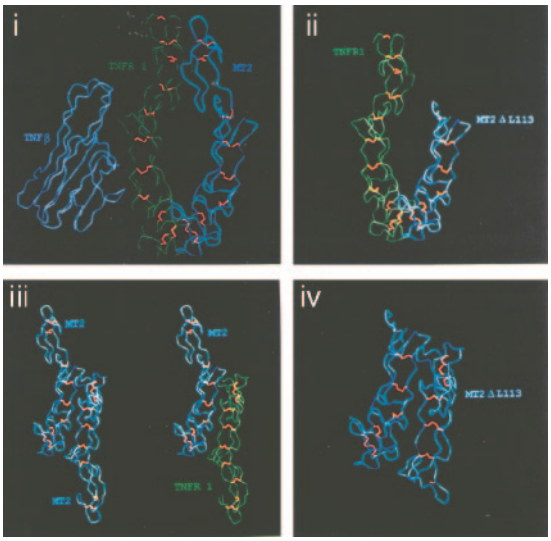

FIG. 7. Secondary structural predictions of M-T2 and TNFR. Structural data from human TNFR1 (green) were used to generate a predicted secondary structure for the N-terminal region of M-T2 (blue). Identical residues were given the same structural constraints as in TNFR1, but nonidentical residues were weighted less stringently. Panels: i, TNF-β bound to a parallel TNFR1:M-T2 dimer; ii, TNFR1 and M-T2ΔL113 mutein in parallel dimer conformation; iii, M-T2 dimer and M-T2:TNFR1 heterodimer in antiparallel conformation; iv, M-T2ΔL113 dimer in antiparallel conformation.

bioavailable TNF-α which might otherwise affect neighboring uninfected cells or act systemically. Thus, the ability of M-T2 to specifically inhibit human TNFR function indicates its ability to indirectly limit human TNF-α. In this sense, M-T2 vPLAD confers intracellular M-T2 with a potent species nonspecific inhibitory activity against both TNF-α and TNFR, while secreted M-T2 inhibits only soluble TNF-α and acts in a strictly species-specific manner (38). Therefore, M-T2 is a "dominant-negative" inhibitor that appears to be acting in a manner somewhat similar to that recently ascribed to TRAIL-R4 PLAD in inhibiting TRAIL-R2-mediated cell death (10).

Modeling of a predicted secondary structure of M-T2 together with the known secondary structure of TNFRs (30) illustrates how M-T2 might exert its TNFR-inhibitory activity (Fig. 7). These modeling predictions suggest that the N-terminal TNFR-homologous region of M-T2 is structurally similar to the N-terminal regions of human TNFRs (Fig. 7). This is consistent with the predicted secondary structures of the N-terminal regions of other TNFR superfamily molecules which are also remarkably similar (32). Because the extracellular regions of TNFRs have been found as parallel and antiparallel dimers (30), it is possible that T2 can form heterocomplexes in either of these conformations. The antiparallel conformation is found under low-pH conditions, which are thought to mimic the environment in intracellular compartments. The modeling predictions indicate that antiparallel T2-TNFR heterocomplexes would share considerably more surface interface than a parallel T2-TNFR heterocomplex (Fig. 7) and thus predicts that M-T2 occurs in an antiparallel conformation with cellular TNFR within intracellular vesicles, where we find these molecules colocalized (Fig. 5). However, this model also potentially explains how even the most severely truncated M-T2 protein, T2ΔL113 (which we described previously [40, 41]), retains its antiapoptotic function, as it likely retains a strong propensity to stably associate with TNFR in an antiparallel, apoptotic signaling-incompetent conformation (Fig. 7). These modeling predictions are consistent with our experimental data, but further experiments, such as with FRET technology and C- and N-tagged proteins, are needed to confirm these hypotheses. Nevertheless, our data clearly suggest that when bound to M-T2, TNFRs are in a conformation that is nonconducive to death signaling. TNFR1 transduces a number of other signaling pathways in addition to caspase-mediated apoptotic signaling; TNFR1 can transduce activation of NFκB, Jun, and MAP kinase, and TNFR1 induces neutral and acid sphingomyelinase, resulting in the production of ceramide (55). Recent evidence suggests that these pathways appear to be tightly regulated by TNFR internalization (36). Our data indicate that M-T2 prevents TNFR1-induced apoptotic signaling from intracellular locations, and in this regard it will be interesting to determine whether M-T2 affects the recruitment of particular TNFR1-association proteins and hence other TNFR1 signaling pathways.

It is clear that apoptosis is an innate response to virus infection, and in many situations this necessitates that viruses express multiple antiapoptotic proteins in order to maintain cellular viability for long enough periods to sustain productive virus replication in different cell types (31). Apoptosis of virus-infected parenchymal cells can dramatically influence the virus burden, and apoptosis of virus-infected lymphocytes is thought to be a key event controlling the dissemination of lymphotropic virus in vivo. However, in many cases the trigger(s) that initiates virus-induced apoptosis has not been defined. We have demonstrated that M-T2 protects against virus-induced lymphocyte apoptosis (24) and specifically inhibits TNFR1-mediated cell death. The fact that viruses encode proteins that act to subvert nearly all aspects of TNFR signaling (5, 6, 42) emphasizes the importance of the TNF-α/TNFR axis in antiviral immunity and virus-host interactions. Indeed, it is particularly noteworthy that there is virtually no detectable alteration in gene expression of TNFR or TNFR signaling molecules in variola virus (smallpox virus)-infected cells, which strongly implies that variola virus employs a nontranscriptional and nontranslational strategy to inhibit these pathways (35). We have identified a vPLAD within all poxvirus T2-like vTNFR ORFs and demonstrated that it is required for M-T2's inhibition of TNFR-induced death without altering TNFR expression levels. Given that the vPLAD is also present within variola virus G2R, these T2-like proteins are prime candidates for mediating variola virus's subversion of the TNFR axis. It is unknown whether other vTNFR molecules, such as the poxvirus CrmB, -C, -D, and -E proteins, vCD30, and human cytomegalovirus UL144, act in an analogous manner to M-T2 by forming inhibitory complexes with their cellular homologues TNFR, LTβR, CD30, and HVEM, but this can easily be tested. Finally, the demonstrated role of N-terminal vPLAD as critical for the inhibition of TNFR signaling confirms that this is a functional region within the ectodomain of TNFRs that regulates TNFR biology, and notably, it is distinct from the ligand-binding domain which resides within CRD2 and CRD3 (8, 41, 42). The M-T2 vPLAD spans amino acids 18 to 52, which lies within CRD1, and this is entirely analogous to the situation

already demonstrated for PLAD in human TNFR and Fas receptors (11, 48). Furthermore, for Fas, dominant interfering mutations are only effective when this N-terminal PLAD of CRD1 is intact (48). Finally, targeting cellular PLAD function by recombinant protein mimotopes or humanized monoclonal antibodies is likely to be efficacious clinically in any disease in which anti-TNF-α-based therapies are currently used, and in fact, cellular "PLAD-only" proteins have recently been demonstrated to have clinical efficacy in murine models of experimental inflammatory arthritis (11). Therefore, this study not only defines a novel mechanism of viral subversion of TNF-α/TNFR biology, but it also substantiates the targeting the TNFR PLAD in the development of the next generation of anti-TNF-α/TNFR-based therapeutics.

ACKNOWLEDGMENTS

We thank Bruce Seet and Colin Macauley (Robarts Research Institute) for help in generating T2-specific antibody; Kathryn Bateman (University of Alberta) for T2 predicted structures; Sabine Piller, Helen Rizos, and Monica Miranda-Saksena (Westmead Millennium Institute) for antibody reagents; Jacqui Mills (Westmead Millennium Institute) for technical assistance with confocal microscopy; and Peter Kerr (CSIRO, Australia) for thoughtful comments on the biology of myxoma virus infection.

F.K.-M.C. is supported by NIH grant AI065877 and a Cancer Research Institute investigator award. This work was supported by CIHR and NCIC grants to G.M. and a University of Sydney U2000 fellowship and NH&MRC (Australia) project grant 211128 to L.S.

REFERENCES

1. **Afonso, C. L., E. R. Tulman, Z. Lu, L. Zsak, N. T. Sandybaev, U. Z. Kerembekova, V. L. Zaitsev, G. F. Kutish, and D. L. Rock.** 2002. The genome of camelpox virus. Virology **295:**1–9.
2. **Alcami, A., A. Khanna, N. L. Paul, and G. L. Smith.** 1999. Vaccinia virus strains Lister, USSR and Evans express soluble and cell-surface tumour necrosis factor receptors. J. Gen. Virol. **80:**949–959.
3. **Aragane, Y., D. Kulms, D. Metze, G. Wilkes, B. Poppelmann, and T. A. Luger.** 1998. Ultraviolet light induces apoptosis via direct activation of CD95 (Fas/APO-1) independently of its ligand CD95L. J. Cell Biol. **140:**171–182.
4. **Barry, M., S. Hnatiuk, K. Mossman, S. F. Lee, L. Boshkov, and G. McFadden.** 1997. The myxoma virus M-T4 gene encodes a novel RDEL-containing protein that is retained within the endoplasmic reticulum and is important for the productive infection of lymphocytes. Virology **239:**360–377.
5. **Benedict, C. A., T. A. Banks, and C. F. Ware.** 2003. Death and survival: viral regulation of TNF signaling pathways. Curr. Opin. Immunol. **15:**59–65.
6. **Benedict, C. A., P. S. Norris, and C. F. Ware.** 2002. To kill or be killed: viral evasion of apoptosis. Nat. Immunol. **3:**1013–1018.
7. **Cameron, C., S. Hota-Mitchell, L. Chen, J. Barrett, J.-X. Cao, C. Macaulay, D. Willer, D. Evans, and G. McFadden.** 1999. The complete DNA sequence of myxoma virus. Virology **246:**298–318.
8. **Chan, F. K., H. J. Chun, L. Zheng, R. M. Siegel, K. L. Bui, and M. J. Lenardo.** 2000. A domain in TNF receptors that mediates ligand-independent receptor assembly and signaling. Science **288:**2351–2354.
9. **Chen, N., M. I. Danila, Z. Feng, R. M. Buller, C. Wang, X. Han, E. J. Lefkowitz, and C. Upton.** 2003. The genomic sequence of ectromelia virus, the causative agent of mousepox. Virology **317:**165–186.
10. **Clancy, L., K. Mruk, K. Archer, M. Woelfel, J. Mongkolsapaya, G. Screaton, M. J. Lenardo, and F. K.-M. Chan.** 2005. Preligand assembly domain-mediated ligand-independent association between TRAIL receptor 4 (TR4) and TR2 regulates TRAIL-induced apoptosis. Proc. Natl. Acad. Sci. USA **102:**18099–18104.
11. **Deng, G.-M., L. Zheng, F. K.-M. Chan, and M. Lenardo.** 2005. Amelioration of inflammatory arthritis by targetting the pre-ligand assembly domain of tumour necrosis factor receptors. Nat. Med. **11:**1304.
12. **Dougall, W. C., M. Glaccum, K. Charrier, K. Rohrbach, K. Brasel, T. De Smedt, E. Daro, J. Smith, M. E. Tometsko, C. R. Maliszewski, A. Armstrong, V. Shen, S. Bain, D. Cosman, D. Anderson, P. J. Morrissey, J. J. Peschon, and J. C. Schuh.** 1999. RANK is essential for osteoclast and lymph node development. Genes Dev. **13:**2412–2424.
13. **Everett, H., M. Barry, S. F. Lee, X. Sun, K. Graham, J. Stone, R. C. Bleackley, and G. McFadden.** 2000. M11L: a novel mitochondria-localized protein of myxoma virus that blocks apoptosis of infected leukocytes. J. Exp. Med. **191:**1487–1498.
14. **Filippova, M., H. Song, J. L. Connolly, T. S. Dermody, and P. J. Duerksen-Hughes.** 2002. The human papillomavirus 16 E6 protein binds to tumor necrosis factor (TNF) R1 and protects cells from TNF-induced apoptosis. J. Biol. Chem. **277:**21730–21739.
15. **Friedman, J. M., and M. S. Horwitz.** 2002. Inhibition of tumor necrosis factor alpha-induced NF-κB activation by the adenovirus E3-10.4/14.5K complex. J. Virol. **76:**5515–5521.
16. **Goebel, S. J., G. P. Johnson, M. E. Perkus, S. W. Davis, J. P. Winslow, and E. Paoletti.** 1990. The complete DNA sequence of vaccinia virus. Virology **179:**247–266.
17. **Gorman, H.** 1985. High efficiency gene transfer into mammalian cells, p. 143–165. *In* D. M. Glover (ed.), DNA cloning. IRL Press, Oxford, United Kingdom.
18. **Griffith, T. S., C. T. Rauch, P. J. Smolak, J. Y. Waugh, N. Boiani, D. H. Lynch, C. A. Smith, R. G. Goodwin, and M. Z. Kubin.** 1999. Functional analysis of TRAIL receptors using monoclonal antibodies. J. Immunol. **162:**2597–2605.
19. **Guerin, J. L., J. Gelfi, S. Boullier, M. Delverdier, F. A. Bellanger, S. Bertagnoli, I. Drexler, G. Sutter, and F. Messud-Petit.** 2002. Myxoma virus leukemia-associated protein is responsible for major histocompatibility complex class I and Fas-CD95 down-regulation and defines scrapins, a new group of surface cellular receptor abductor proteins. J. Virol. **76:**2912–2923.
20. **Harlow, E., and D. Lane.** 1988. Antibodies: a laboratory manual. Cold Spring Harbor Laboratory Press, Cold Spring Harbor, N.Y.
21. **Jones, S. J., E. C. Ledgerwood, J. B. Prins, J. Galbraith, D. R. Johnson, J. S. Pober, and J. R. Bradley.** 1999. TNF recruits TRADD to the plasma membrane but not the trans Golgi network, the principal subcellular location of TNF-R1. J. Immunol. **162:**1042–1048.
22. **Juo, P., C. J. Kuo, J. Yuan, and J. Blenis.** 1998. Essential requirement for caspase-8/FLICE in the initiation of the Fas-induced apoptotic cascade. Curr. Biol. **10:**1001–1008.
23. **Kothny-Wilkes, G., D. Kulms, T. A. Luger, M. Kubin, and T. Schwarz.** 1999. Interleukin-1 protects transformed keratinocytes from tumor necrosis factor-related apoptosis-inducing ligand- and CD95-induced apoptosis but not from ultraviolet radiation-induced apoptosis. J. Biol. Chem. **274:**28916–28921.
24. **Macen, J. L., K. A. Graham, S. F. Lee, M. Schreiber, L. K. Boshkov, and G. McFadden.** 1996. Expression of the myxoma virus tumor necrosis factor receptor homologue and M11L genes is required to prevent virus-induced apoptosis in infected rabbit T lymphocytes. Virology **218:**232–237.
25. **Mansouri, M., E. Bartee, K. Gouveia, B. T. Hovey Nerenberg, J. Barrett, L. Thomas, G. Thomas, G. McFadden, and K. Fruh.** 2003. The PHD/LAP-domain protein M153R of myxomavirus is a ubiquitin ligase that induces the rapid internalization and lysosomal destruction of CD4. J. Virol. **77:**1427–1440.
26. **Massung, R. F., L. I. Liu, J. Qi, J. C. Knight, T. E. Yuran, A. R. Kerlavage, J. M. Parsons, J. C. Venter, and J. J. Esposito.** 1994. Analysis of the complete genome of smallpox variola major virus strain Bangladesh—1975. Virology **201:**215–240.
27. **Mein, E., H. Fickenscher, M. Thome, J. Tschopp, and B. Fleckenstein.** 1998. Anti-apoptotic strategies of lymphotropic viruses. Immunol. Today **19:**474–479.
28. **Messud-Petit, F., J. Gelfi, M. Delverdier, M. F. Amardeilh, R. Py, G. Sutter, and S. Bertagnoli.** 1998. Serp2, an inhibitor of the interleukin-1β-converting enzyme, is critical in the pathobiology of myxoma virus. J. Virol. **72:**7830–7839.
29. **Mossman, K., S. F. Lee, M. Barry, L. Boshkov, and G. McFadden.** 1996. Disruption of M-T5, a novel myxoma virus gene member of poxvirus host range superfamily, results in dramatic attenuation of myxomatosis in infected European rabbits. J. Virol. **70:**4394–4410.
30. **Naismith, J. H., T. Q. Devine, T. Kohno, and S. R. Sprang.** 1996. Structures of the extracellular domain of the type I tumor necrosis factor receptor. Structure **4:**1251–1262.
31. **Nash, P., J. Barrett, J. X. Cao, S. Hota-Mitchel, A. S. Lalani, H. Everett, X. M. Xu, J. Robichaud, S. Hnatiuk, C. Ainslie, B. T. Seet, and G. McFadden.** 1999. Immunomodulation by viruses: the myxoma virus story. Immunol. Rev. **168:**103–120.
32. **Peitsch, M. C., and J. Tschopp.** 1995. Comparative molecular modelling of the Fas-ligand and other members of the TNF family. Mol. Immunol. **32:**761–772.
33. **Petit, F., S. Bertagnoli, J. Gelfi, F. Fassy, C. Boucraut-Baralon, and A. Milon.** 1996. Characterization of a myxoma virus-encoded serpin-like protein with activity against interleukin-1β-converting enzyme. J. Virol. **70:**5860–5866.
34. **Rizos, H., A. P. Darmanian, E. A. Holland, G. J. Mann, and R. F. Kefford.** 2001. Mutations in the INK4a/ARF melanoma susceptibility locus functionally impair p14ARF. J. Biol. Chem. **276:**44.
35. **Rubins, K. H., L. E. Hensley, P. B. Jahrling, A. R. Whitney, T. W. Geisbert, J. W. Huggins, A. Owen, J. W. Leduc, P. O. Brown, and D. A. Relman.** 2004. The host response to smallpox: analysis of the gene expression program in peripheral blood cells in a nonhuman primate model. Proc. Natl. Acad. Sci. USA **101:**15190–15195.
36. **Schneider-Brachert, W., V. Tchikov, J. Neumeyer, M. Jakob, S. Winoto-Morbach, J. Feindt, M. Henrich, O. Merkel, M. Ehrenschwender, D. Adam,**

R. Mentlein, D. Kabelitz, and S. Schutze. 2004. Compartmentalization of TNF receptor 1 signalling: internalized TNF receptorsomes as death signaling vesicles. Immunity **21:**415–428.

37. **Schreiber, M., and G. McFadden.** 1996. Mutational analysis of the ligand-binding domain of M-T2 protein, the tumor necrosis factor receptor homologue of myxoma virus. J. Immunol. **157:**4486–4495.
38. **Schreiber, M., and G. McFadden.** 1994. The myxoma virus TNF-receptor homologue (T2) inhibits tumor necrosis factor-alpha in a species-specific fashion. Virology **204:**692–705.
39. **Schreiber, M., K. Rajarathnam, and G. McFadden.** 1996. Myxoma virus T2 protein, a tumor necrosis factor (TNF) receptor homolog, is secreted as a monomer and dimer that each bind rabbit TNFα, but the dimer is a more potent TNF inhibitor. J. Biol. Chem. **271:**13333–13341.
40. **Schreiber, M., L. Sedger, and G. McFadden.** 1997. Distinct domains of M-T2, the myxoma virus tumor necrosis factor (TNF) receptor homolog, mediate extracellular TNF binding and intracellular apoptosis inhibition. J. Virol. **71:**2171–2181.
41. **Sedger, L., and G. McFadden.** 1996. M-T2: a poxvirus TNF receptor homologue with dual activities. Immunol. Cell Biol. **74:**538–545.
42. **Sedger, L. M.** 2005. Viral inhibition of tumour necrosis factor-α (TNFα) and TNF-receptor induced apoptosis and inflammation. Curr. Med. Chem.-Anti-Inflamm. Anti-Allergy Agents **4:**597–615.
43. **Sedger, L. M., D. M. Shows, R. A. Blanton, J. J. Peschon, R. G. Goodwin, D. Cosman, and S. R. Wiley.** 1999. IFN-γ mediates a novel antiviral activity through dynamic modulation of TRAIL and TRAIL receptor expression. J. Immunol. **163:**920–926.
44. **Shchelkunov, S. N., A. V. Totmenin, I. V. Babkin, P. F. Safronov, O. I. Ryazankina, N. A. Petrov, V. V. Gutorov, E. A. Uvarova, M. V. Mikheev, J. R. Sisler, J. J. Esposito, P. B. Jahrling, B. Moss, and L. S. Sandakhchiev.** 2001. Human monkeypox and smallpox viruses: genomic comparison. FEBS Lett. **509:**66–70.
45. **Shchelkunov, S. N., A. V. Totmenin, V. N. Loparev, P. F. Safronov, V. V. Gutorov, V. E. Chizhikov, J. C. Knight, J. M. Parsons, R. F. Massung, and J. J. Esposito.** 2000. Alastrim smallpox variola minor virus genome DNA sequence. Virology **266:**361–386.
46. **Sheikh, M. S., M. J. Antinore, Y. Huang, and A. J. J. Fornace.** 1998. Ultraviolet irradiation-induced apoptosis is mediated via ligand independent activation of tumor necrosis factor receptor 1. Oncogene **17:**2555–2563.
47. **Shisler, J., C. Yang, B. Walter, C. F. Ware, and L. R. Gooding.** 1997. The adenovirus E3-10.4K/14.5K complex mediates loss of cell surface Fas (CD95) and resistance to Fas-induced apoptosis. J. Virol. **71:**8299–8306.
48. **Siegel, R., J. K. Frederiksen, D. A. Zacharias, F. K.-M. Chan, M. Johnson, D. Lynch, R. Y. Tsien, and M. J. Lenardo.** 2000. Fas preassociation required for apoptosis signalling and dominant inhibition by pathogenic mutations. Science **288:**2354–2357.
49. **Smith, C. A., T. Davis, J. M. Wignall, W. S. Din, T. Farrah, C. Upton, G. McFadden, and R. G. Goodwin.** 1991. T2 open reading frame from the Shope fibroma virus encodes a soluble form of the TNF receptor. Biochem. Biophys. Res. Commun. **176:**335–342.
50. **Tobin, D., M. van Hogerlinden, and R. Toftgard.** 1998. UVB-induced association of tumor necrosis factor (TNF) receptor 1/TNF receptor-associated factor-2 mediates activation of Rel proteins. Proc. Natl. Acad. Sci. USA **95:**565–569.
51. **Tollefson, A. E., T. W. Hermiston, D. L. Lichtenstein, C. F. Colle, R. A. Tripp, T. Dimitrov, K. Toth, C. E. Wells, P. C. Doherty, and W. S. Wold.** 1998. Forced degradation of Fas inhibits apoptosis in adenovirus-infected cells. Nature **392:**726–730.
52. **Tollefson, A. E., K. Toth, K. Doronin, M. Kuppuswamy, O. A. Doronina, D. L. Lichtenstein, T. W. Hermiston, C. A. Smith, and W. S. Wold.** 2001. Inhibition of TRAIL-induced apoptosis and forced internalization of TRAIL receptor 1 by adenovirus proteins. J. Virol. **75:**8875–8887.
53. **Upton, C., A. M. DeLange, and G. McFadden.** 1987. Tumorigenic poxviruses: genomic organization and DNA sequence of the telomeric region of the Shope fibroma virus genome. Virology **160:**20–30.
54. **Upton, C., J. L. Macen, M. Schreiber, and G. McFadden.** 1991. Myxoma virus expresses a secreted protein with homology to the tumor necrosis factor receptor gene family that contributes to viral virulence. Virology **184:**370–382.
55. **Wajant, H., K. Pfizenmaier, and P. Scheurich.** 2003. Tumor necrosis factor signaling. Cell Death Differ. **10:**45–65.
56. **Walczak, H., R. E. Miller, K. Ariail, B. Gliniak, T. S. Griffith, M. Kubin, W. Chin, J. Jones, A. Woodward, T. Le, C. Smith, P. Smolak, R. G. Goodwin, C. T. Rauch, J. C. Schuh, and D. H. Lynch.** 1999. Tumoricidal activity of tumor necrosis factor-related apoptosis-inducing ligand in vivo. Nat. Med. **5:**157–163.
57. **Willer, D. O., G. McFadden, and D. H. Evans.** 1999. The complete sequence of Shope (rabbit) fibroma virus. Virology **264:**319–343.
58. **Xu, X., P. Nash, and G. McFadden.** 2000. Myxoma virus expresses a TNF receptor homolog with two distinct functions. Virus Genes **21:**97–109.